Published in final edited form as:

Cells Tissues Organs. 2018 ; 205(4): 197–207. doi:10.1159/000490884.

Effects of dexamethasone dose and timing on tissue-engineered skeletal muscle units

Alexie A. Larson[1], **Brian C. Syverud**[2], **Shelby E. Florida**[1], **Brittany L. Rodriguez**[2], **Molly N. Pantelic**[1], **Lisa M. Larkin**[1,2]

[1]Molecular and Integrative Physiology, University of Michigan, 2025 BSRB, 109 Zina Pitcher Place, Ann Arbor, MI, 48109-2200

[2]Biomedical Engineering, University of Michigan, 2025 BSRB, 109 Zina Pitcher Place, Ann Arbor, MI, 48109-2200

Abstract

Our lab showed that administration of dexamethasone (DEX) stimulates myogenesis and results in advanced structure in our engineered skeletal muscle units (SMUs). While administration of 25nM DEX resulted in the most advanced structure, 10nM dosing resulted in the greatest force production. We hypothesized that administration of 25nM DEX during the entire fabrication process was toxic to the cells and that administration of DEX at precise time points during myogenesis would result in SMUs with more advanced structure and function. Thus, we fabricated SMUs with 25nM DEX administered at early proliferation (days 0–4), late proliferation (days 3–5), and early differentiation (days 5–7) stages of myogenesis and compared them to SMUs treated with 10nM DEX (days 0–16). Cell proliferation was measured with a BrdU assay (day 4) and myogenesis was examined by immunostaining for MyoD (day 4), myogenin (day 7), and α-actinin (day 11). Following SMU formation, isometric tetanic force production was measured. Analysis of cell proliferation indicated that 25nM DEX administered at early proliferation (days 0–4) provided 21.5% greater myogenic proliferation than 10nM DEX (days 0–4). In addition, 25nM DEX administered at early differentiation (days 5–7) showed the highest density of myogenin-positive cells demonstrating the greatest improvement in differentiation of myoblasts. However, the most advanced sarcomeric structure and highest force production was exhibited with sustained administration of 10nM DEX (days 0–16). In conclusion, altering the timing of 25nM DEX administration did not enhance the structure or function of our SMUs. SMUs were optimally fabricated with sustained administration of 10nM DEX.

Keywords

tissue-engineering; skeletal muscle; satellite cells; dexamethasone

Corresponding Author: Lisa Larkin, PhD, Associate Professor, Molecular and Integrative Physiology, Biomedical Engineering, University of Michigan, Biomedical Science Research Building (BSRB), 109 Zina Pitcher Place, Room #2025, 48109-2200, Phone: (734) 936-8181, Fax: (734) 615-3292, llarkin@umich.edu.

Contributions:

A.A.L., B.C.S., and L.M.L designed the study; A.A.L., B.C.S., S.E.F., and B.L.R. acquired the data, A.A.L. and M.N.P. analyzed the data; A.A.L, B.C.S., S.E.F., B.L.R., and L.M.L wrote and revised the manuscript.

Author Disclosure Statement

The authors have no competing financial interests.

Introduction

Volumetric muscle loss (VML), a traumatic loss of skeletal muscle that overwhelms the body's native repair mechanism and results in functional impairment, necessitates surgical intervention [VanDusen et al., 2014]. Limitations to current VML treatments, including donor site morbidity and graft tissue availability, present a need for exogenous graft muscle sources [Mertens et al., 2015]. Tissue-engineered skeletal muscle technologies represent a promising graft source for muscle loss repair [Larkin et al., 2006]. However, engineered muscle to date produces forces that are substantially lower than adult muscle, limiting its potential for repair [Williams et al., 2013]. In order for engineered muscle to become a viable means of treating VML, it is essential to advance structural maturity and force production of engineered skeletal muscle towards an adult muscle phenotype. To fabricate phenotypically mature muscle, tissue engineers have used growth factors known to regulate myogenesis *in vivo* [Allen and Boxhorn, 1989]. Specifically, media is supplemented with growth factors that promote myogenic proliferation, myoblast differentiation, and myotube formation [Husmann et al., 1996]. These studies have shown that providing the appropriate cues to improve each stage of myogenesis is necessary to engineer skeletal muscle with optimal regenerative and functional potential.

Due to their influence on metabolic processes regulating muscle mass and size, glucocorticoids show promise in providing biochemical cues to enhance the structure and function of engineered skeletal muscle [Morgan et al., 2016]. The effects of dexamethasone (DEX), a synthetic glucocorticoid, have been previously analyzed *in vitro* with supplementation to myoblast cell lines or muscle cell isolates, as well as *in vivo* through injection or oral administration; however, the application of DEX in skeletal muscle tissue engineering has yet to be fully explored [Belanto et al., 2010; Syverud et al., 2016; Inder et al., 2010]. At supraphysiological doses, approximately 10,000 nM in adult human skeletal muscle and 100 nM in myogenic cell lines, DEX induces skeletal muscle atrophy through increased production of myostatin, a negative regulator of myogenesis, and decreased production of IGF-1, a hormone that stimulates muscle mass [Qin et al., 2013; Inder et al., 2010]. Specifically, upregulating myostatin decreases satellite cell proliferation and differentiation, while downregulating IGF-1 inhibits the PI3-kinase/Akt pathway resulting in stimulation of the FOX03 transcription factor and downstream ubiquitin ligases, MuRF1 and atrogin-1 [Kuo et al., 2012; Giorgino and Smith, 1995]. Eventually, these modifications in myostatin and IGF-1 production stimulate protein degradation, which produces muscle atrophy [Schakman et al., 2008]. Furthermore, researchers have found that addition of pharmacologic doses of DEX to C2C12 murine myoblast cells can inhibit cell proliferation and protein synthesis processes, which hinder myoblast differentiation and myotube fusion [Belanto et al., 2010]. Interestingly, at similar doses, DEX can augment production of dysferlin, a calcium binding transmembrane protein involved in membrane fusion and repair, which promotes myogenic differentiation and enhances myogenic fusion [Desler et al., 2014]. Overall, the diverse effects observed with DEX administration demonstrate the importance of controlling dose and timing when enhancing *in vitro* conditions for engineering skeletal muscle.

Previous studies from our lab revealed that sustained administration of 10 nM DEX (days 0–16) yields SMUs with the most advanced form and function to date [Syverud et al., 2016]. Specifically, sustained administration of 10 nM DEX produced SMUs with advanced structural development in sarcomeric structure and a five-fold increase in isometric force production relative to no DEX controls [Syverud et al., 2016]. Although this study indicated that sustained administration of 25 nM DEX improved myogenic proliferation and differentiation, force production in these skeletal muscle units (SMUs) was lower and blebbing, an indicator of cell death, was increased compared to SMUs without DEX [Syverud et al., 2016]. Therefore, we hypothesized that administration of 25 nM DEX during the entire fabrication process was toxic to the cells and that administration at precise time points during development, rather than sustained administration, would result in the most advanced structure and function. To test our hypothesis, we added 25 nM DEX at early proliferation (days 0–4), late proliferation (days 3–5), and early differentiation (days 5–7) stages, and evaluated myogenic proliferation, differentiation, structural maturation, and force production. We aimed to reproduce the improvements in myogenesis observed with administration of 25 nM DEX early in development and determine whether restricting the administration of 25 nM DEX to one precise stage of myogenesis would produce SMUs with improved force production compared to SMUs with sustained administration of 10 nM DEX. Overall, we aimed to determine the optimal time to administer the 25 nM DEX dose during our SMU fabrication process, with the goal of improving our engineered skeletal muscle for therapeutic purposes.

Materials and Methods

Animal model and animal care

Engineered skeletal muscle was fabricated using soleus muscle isolates and bone marrow from 140 to 160 g female Fischer 344 rats 4 to 6 months of age, obtained from Charles River Laboratories, Inc. (Wilmington, MA). All animals were acclimated to colony conditions for 1 week before any procedure. Animals were fed Purina Rodent Chow 5001 and water *ad libitum*. All dissection procedures we performed in an aseptic environment, while animals were in a deep plane of anesthesia induced by intraperitoneal injections of sodium pentobarbital (65 mg/kg). Supplemental doses of pentobarbital were administered as required to maintain an adequate depth of anesthesia. All animal care and animal surgery procedures were in accordance with *The Guide for Care and Use of Laboratory Animals* [National Research Council, 1996]; the protocol was approved by the University Committee for the Use and Care of Animals.

Dissection of muscle and isolation of muscle cells

Both rat soleus muscles were removed under aseptic conditions and sterilized in 70% ethanol. Prior to dissociation, the muscles were incubated in 5 mL of transport medium consisting of Dulbecco's phosphate-buffered saline (DPBS [pH 7.2]; cat. No. 14190–144; Gibco BRL) with 2% antibiotic-antimycotic (ABAM; Cat. No. 15240–062; Gibco BRL) for 5 min. The muscles were then minced using a razor blade, placed under ultraviolet light for 15 min in 15 mL Ham's F12 (cat. No. 11765–047; Gibco BRL), and added to a dissociation solution consisting of 32 U dispase (1.8 U/mg, cat. No. 17105–041; Gibco BRL) and 2390 U

type IV collagenase (239 U/mg, cat. No. 17104–019; Gibco BRL) in 20 mL of Ham's F12 nutrient media. The mixture was then kept at 37°C with agitation for 90 min to allow the minced muscle to dissociate. The solution was then poured through a 100 μm filter and centrifuged. The dissociation solution was aspirated off and the cells were resuspended in muscle growth medium (MGM).

SMU formation and DEX addition

SMUs were fabricated in individual coated 60 mm polystyrene plates (BD Falcon, Franklin Lakes, NJ), and immunocytochemistry (ICC) was performed on 35 mm plates as described previously [Syverud et al., 2016]. Briefly, a substrate of Sylgard (type 184 silicon elastomer; Dow Chemical Corp., Midland, MI) was cured onto each plate, followed by coating with laminin (Natural Mouse Laminin: Cat No. 23017–015; Gibco BRL, Carlsbad, CA) at 1 mg/cm^2. Following enzymatic dissociation of satellite cells and fibroblasts from rat soleus muscles, the cell isolation mixture was plated in MGM at a density of 600,000 cells per 60 mm plate and 150,000 cells per 35 mm plate. MGM was composed of 60% F-12 Kaighn's modification nutrient mixture (Cat. No. 21127–022; Gibco BRL), 24% Dulbecco's modified Eagle's medium (DMEM; Cat. No. 11995–065; Gibco BRL), 15% fetal bovine serum (FBS; Cat. No. 10437–028; Gibco BRL), and 1% ABAM and was supplemented with 2.4 ng/mL basic fibroblast growth factor (Cat. No. 100–18B; Peprotech, Rocky Hill. NJ).

After the initial plating, cells were left to adhere for either 3 or 4 days, depending on the timing of DEX administration. Plates were subsequently fed MGM every 2 days until fully confluent, as indicated by elongated myotube networks across the base of the plate. At this point, the media were switched to muscle differentiation medium (MDM). MDM was composed of 70% M199 (Cat. No. 11150–059; Gibco BRL), 23% DMEM, 6% FBS, and 1% ABAM and was supplemented with 1 μL/mL insulin-transferrin selenium-X (Cat. No. I1884; Sigma-Aldrich, St. Louis, MO) and 14.4 μg/mL ascorbic acid 2-phosphate. After approximately a week on MDM, resupplied every other day, the monolayers were manually delaminated from the plates using a cell scraper, rolled into cylindrical muscle constructs, and were held at a length of 3 cm by engineered bone anchors fabricated from isolated rat bone marrow cells as described previously [VanDusen et al., 2014].

During the SMU fabrication process, described in Figure 1, 25 nM DEX was added to the media at three different time points: early proliferation (days 0–4), late proliferation (days 3–5), and early differentiation (days 5–7). In addition, sustained addition of 10 nM DEX was used as a control, which involved supplemental doses of 10 nM DEX to be added with each media change. The three time points were chosen to optimize the use of 25 nM DEX in enhancing isolated cell proliferation, differentiation, and maturation of the delaminating monolayer and subsequent 3-D SMU, respectively.

Immunocytochemical analysis

During SMU fabrication, a subset of the plates from each experimental group was fixed in 20°C methanol for 10 min and set aside for ICC. Briefly, the plates were washed for 15 min in 0.1% Triton X-100 (Cat. No. T8787; Sigma) in DPBS (PBST) and blocked with PBST containing 3% bovine serum albumin (PBST-S; Cat. No. A2153; Sigma) for 30 minutes at

4°C. The plates were then incubated overnight at 4°C with the primary antibodies diluted in PBST-S. The primary antibodies were used to detect the presence of BrdU (biotin conjugated sheep polyclonal antibody; Cat. No. ab2284; Abcam, Cambridge, MA), MyoD (mouse monoclonal antibody 1:100 dilution; Cat. No. 554130; BD Biosciences, San Jose, CA), myogenin (rabbit polyclonal antibody 1:50 dilution; Cat. No. sc-576, Santa Cruz Biotechnology, Dallas, TX), and α-actinin (mouse monoclonal antibody 1:200 dilution; Cat. No. A7752; Sigma). Plates stained with antibodies for BrdU had previously been incubated for 24 hours with a BrdU labeling reagent (1:500 dilution; Cat. No. 000103; Life Technologies, Carlsbad, CA) in the culture media. Following three washes in PBST, samples were incubated in 1:500 dilutions of Alexa Fluor anti-mouse, anti-rabbit, or streptavidin secondary antibodies (Life Technologies) for 3 hours at room temperature. Following three washes in PBST, samples were preserved in Prolong Gold with DAPI (Cat. No. P36935; Life Technologies) and cover slipped. The samples were examined and photographed with a Leica Inverted Microscope, and images were analyzed using the Image J software package (NIH, Bethesda, MD, USA).

For ICC analysis, plates (n=6) from each experimental group were fixed and stained (on day 4 for BrdU and MyoD; day 7 for myogenin; and day 11 for α-actinin). From each plate, 10 areas of 0.6 mm^2 were randomly selected and imaged, and the number of positively stained nuclei in each image was counted. Cell proliferation was calculated as a percentage of MyoD-positive nuclei out of BrdU-expressing nuclei. Differentiation of myoblasts into myotubes was determined by measuring the quantity of myogenin-positive cells on each image. To calculate myotube fusion index from the α-actinin images, the number of nuclei associated with an α-actinin-positive myotube containing 4 or more nuclei was divided by the total number of nuclei associated with α-actinin-positive cells.

Myotube size and density

Fourteen days after initial plating of isolated cells, light micrographs of the developing monolayers in each experimental group were captured and analyzed. Specifically, 5 areas of 1.4 mm^2 from each 60 mm plate (n=9) were randomly selected and imaged. Every myotube from these images was then measured in ImageJ to determine its diameter (μm) and the overall density of the myotube network.

SMU contractile measurements

Contractile properties of SMUs (n=12 for 10 nM DEX group, n=9 for each 25 nM DEX group) were measured following roll-up into cylindrical form. The protocol for measuring contractility of engineered muscle constructs has been described previously [Larkin et al., 1998; Dennis and Kosnik, 2000]. Briefly, the pin on one end of the SMU was raised from the Sylgard and attached to an optical force transducer with a load range of 0 to 5 mN (SI-BAM21-LC KG7A; World Precision Instruments, Sarasota, FL). Platinum wire electrodes were placed along either side of the SMU for electrical field stimulation. The temperature of the construct was maintained at 37°C, using a heated aluminum platform. Twitch contractions were elicited using a single 2.5 ms pulse at 60 and 90 mA, whereas tetanic force was determined using a 1 s train of 2.5 ms pulses at 90 mA and 60 and 80 Hz. Data files for each peak twitch force and peak tetanic force trace were recorded and subsequently

analyzed using LabVIEW 2013 (National Instruments, Austin, TX). Time to peak tension (TPT) was defined as the amount of time from baseline to peak tetanus, and half relaxation rate (½ RT) was defined as the amount of time from the onset of relaxation to half of peak tetanus.

Transmission electron microscopy analysis

Following measures of mechanical function, SMUs were fixed overnight at room temperature in 0.1M phosphate buffer (Fisher Scientific, Pittsburgh, PA, USA, cat. no. S369–500) containing 2.5% glutaraldehyde (Electron Microscopy Sciences, Hatfield, PA, USA, cat no. 16210), post-fixed at 4°C for one hour in 0.1M phosphate buffer containing 1% osmium tetroxide (Electron Microscopy Sciences, cat no. 19150), and polymerized in Embed 812 resin (Electron Microscopy Sciences, cat. no. 14900) at 60°C for 24 hours. Ultra-thin 70nm sections were then cut and stained with uranyl acetate (Electron Microscopy Sciences, cat. no. 22400) and lead citrate (Electron Microscopy Sciences, cat. nos. 17900 and 21140) and imaged using a JEOL JEM-1400Plus transmission electron microscope (TEM). Images were used to evaluate structural maturity of SMUs by analysis of the development, density, and alignment of collagen fibers and the organization of Z-disks and muscle fibers.

Statistical analysis

Values are presented as mean ± standard error. Measurements of significant difference between means were performed using GraphPad Prism. Means were compared using either Student t-test when comparing two groups or one-way ANOVA tests with Tukey *post hoc* comparisons. Differences were considered significant at a p-value < 0.05.

Results

Administration of 25 nM DEX results in the greatest increase in committed myogenic progenitors

To determine the effect of DEX dose on the proliferation of isolated myogenic satellite cells, 10 and 25 nM doses of DEX were administered on the day of plating (day 0). On day 4, ICC co-staining of BrdU, a synthetic thymidine analog, and MyoD, a myogenic transcription factor, was used to identify the total number of proliferating cells and the number of proliferating myogenic cells, respectively [Alway et al., 2013; Belanto et al., 2010]. Analysis of the percentage of cells expressing BrdU and MyoD indicates that plates receiving 25 nM DEX at early proliferation (days 0–4) had 21.5% more myogenic cell proliferation on average than the plates receiving 10 nM DEX at early proliferation (87.7±1.7% versus 72.2±2.8%, respectively; Figure 2). The difference in the number of MyoD-expressing cells between the two groups was significant ($p<0.001$). Therefore, the greatest number of proliferating myogenic nuclei was obtained with administration of 25 nM DEX at early proliferation.

Effects of DEX on myoblast differentiation and myotube fusion

The influence of DEX dose and timing on myoblast differentiation into myotubes was evaluated by ICC analysis of myogenin staining on day 7. On average, the administration of

25 nM DEX at early and late stages of proliferation produced myogenin-positive cell densities of 84.2±4.0 and 90.6±11.9 cells/mm^2, respectively, which were both significantly lower than the average myogenin-positive cell density of 127.1±6.4 cells/mm^2 produced with sustained administration of 10 nM DEX (p=0.012 and p=0.036, respectively; Figure 3A). In addition, administration of 25 nM DEX at early and late stages of proliferation produced even lower myogenin-positive cell densities compared to the average myogenin-positive cell density of 150.3±10.3 cells/mm^2 produced with administration of 25 nM DEX at early differentiation (p<0.001 for both stages of proliferation). Furthermore, there was no difference in myogenin expression between sustained administration of 10 nM DEX and administration of 25 nM DEX at early differentiation; however, administration of 25 nM DEX at early differentiation exhibited a 15.4% greater myogenin-positive cell density compared to sustained administration of 10 nM DEX (150.3±10.3 versus 127.1±6.4 myogenin-positive cells/mm^2, respectively). Ultimately, myogenin immunostaining showed that differentiation of myoblasts into myotubes was greatest with administration of 25 nM DEX at early differentiation (days 5–7) and sustained administration of 10 nM DEX (days 0–7).

The role of DEX in terminal differentiation and myotube fusion was examined using staining for α-actinin, a structural protein localized at the Z-disc in skeletal muscle cells [Belanto et al., 2010]. Following immunostaining on day 11, the percentage of DAPI-stained positive nuclei associated with α-actinin-expressing myotubes containing 4 or more nuclei was assessed to calculate a myotube fusion index value. Plates administered 25 nM DEX at late proliferation exhibited an average fusion index of 79.4±3.0%, which was significantly lower than the average fusion indexes of 91.9±0.9% and 91.4±0.9% that were obtained with sustained administration of 10 nM DEX and administration of 25 nM DEX at early differentiation, respectively (p<0.001 for both; Figure 3B). Comprehensively, the most enhanced myoblast differentiation and fusion of myotubes was observed with administration of 25 nM DEX at early differentiation (days 5–7) and sustained administration of 10 nM DEX (days 0–11).

Myotube growth with DEX addition

On day 14, light microscopy images were captured for analysis of myotube size and density of developing monolayers. Measurements of myotube size showed that the average myotube diameter with administration of 25 nM DEX at early and late stages of proliferation was 12.5±0.7 and 11.9±0.7 μm, respectively, which were significantly less than the average myotube diameter of 17.0±1.3 μm obtained with sustained administration of 10 nM DEX (p=0.015 and p=0.005, respectively; Figure 4). Furthermore, the average myotube diameter produced with administration of 25 nM DEX at late proliferation was 32.8% less than the average myotube diameter obtained with administration of 25 nM DEX at early differentiation. The difference in average myotube diameter between administration of 25 nM DEX at late proliferation and administration of 25 nM DEX at early differentiation was significant (p=0.045). However, there was no difference in average myotube diameter between administration of 25 nM DEX at early differentiation and sustained administration of 10 nM DEX (15.8±1.1 versus 17.0±1.3 μm, respectively). Similarly, there were no differences in myotube density between the groups, potentially due to the large intracohort

variability. Again, monolayers with the most robust and greatest density of myotubes were observed with administration of 25 nM DEX at early differentiation (days 5–7) and sustained administration of 10 nM DEX (days 0–14).

Sustained administration of 10 nM DEX enhances structural and contractile properties of SMUs

To evaluate structural maturity of the developing monolayers, immunostaining for α-actinin on day 11 was evaluated. It was evident that plates with sustained administration of 10 nM DEX exhibited advanced sarcomeric structure within muscle fibers that were aligned along the length of the SMU (Figure 5A). TEM images of 3-D SMUs with sustained administration of 10 nM DEX showed large myofibers and an abundance of collagen extracellular matrix (ECM) between myofibers (black asterisks in Figure 5C, E). In addition, sarcomeres in longitudinal and transverse orientation were found in TEM images of SMUs with sustained administration of 10 nM DEX (diamonds in Figure 5E). In contrast to plates with sustained administration of 10 nM DEX, advanced sarcomeric structure was not observed in plates with administration of 25 nM DEX and TEM images of SMUs with administration of 25 nM DEX at early differentiation showed small myofibers and an absence of collagen ECM between myofibers (Figure 5B, D). While no sarcomeres were observed in TEM images of SMUs with administration of 25 nM DEX at early differentiation, there was an abundance of unorganized myofilaments and sparsely organized myofilaments in both longitudinal and transverse orientation along the length of the myofibers (white asterisk in Figure 5D). Furthermore, TEM images of SMUs with administration of 25 nM DEX at early differentiation showed an increase in intracellular lipid droplets, rough endoplasmic reticulum (RER), and nucleoli in myonuclei (small arrowheads, arrows, and large arrowheads in Figure 5D, F). Overall, the greatest advancement in structure was obtained with sustained administration of 10 nM DEX.

Following delamination of 3-D SMUs, contractile properties were measured in response to electrical stimulation. SMUs with administration of 25 nM DEX at early and late stages of proliferation produced average tetanic forces of 39.4±5.2 μN and 67.3±10.6 μN, indicating 73.3% and 54.4% lower force than the average tetanic force of 147.7±31.8 μN produced by SMUs with sustained administration of 10 nM DEX, respectively (Figure 6). The differences in average tetanic force between administration of 25 nM DEX at early and late stages of proliferation and sustained administration of 10 nM DEX were significant ($p=0.004$ and $p=0.045$, respectively). Furthermore, SMUs with administration of 25 nM DEX at early differentiation generated an average tetanic force of 74.9±12.0 μN compared to sustained administration of 10 nM DEX with an average force of 147.7±31.8 μN (49.3% difference); however, the variability within the sustained administration of 10 nM DEX group reduced the ability to identify whether a significant difference between the two groups was present. Similarly, there were no differences in force production between the 25 nM DEX-receiving groups. In addition, the contractile properties, TPT and ½ RT, of the SMUs were measured and no differences were found between the groups (Table 1). Together, the most structurally and functionally mature SMUs were obtained with sustained administration of 10 nM DEX (days 0–16).

Discussion

The purpose of this study was to investigate the myogenic potential of 25 nM DEX by examining the effects *in vitro* following DEX treatment at early proliferation (days 0–4), late proliferation (days 3–5), and early differentiation (days 5–7) stages of myogenesis. We hypothesized that administration of 25 nM DEX during an optimal time point of our fabrication process would yield the greatest advancement in structural and functional properties of our engineered SMUs, exceeding previously evaluated improvements resulting from the administration of sustained 10 nM DEX.

To fabricate SMUs that mimic the phenotype of adult muscle, the early stages of development must be carefully mediated to induce satellite cell proliferation, myoblast differentiation, and myotube fusion. Examination of DEX dose on early proliferation (days 0–4) showed significantly more myogenic cell proliferation with 25 nM DEX compared to 10 nM DEX. In addition, myoblast differentiation was enhanced with administration of 25 nM DEX at early differentiation (days 5–7) and sustained administration of 10 nM DEX (days 0–7) compared to administration of 25 nM DEX at early and late stages of proliferation. The improvement in myoblast differentiation, with administration of 25 nM DEX at early differentiation and sustained administration of 10 nM DEX, translated to the dense monolayers containing myotubes with the greatest fusion indexes and diameters. In addition, visualization of monolayers and electron micrographs of SMUs revealed the greatest advancement in sarcomeric structure with sustained administration of 10 nM DEX; however, electron micrographs of SMUs receiving 25 nM DEX at early differentiation showed increased RER in the cytoplasm of myocytes and increased nucleoli in myonuclei, indicating protein synthesis. Furthermore, the TEM images of SMUs administered 25 nM DEX at early differentiation suggested predominantly myogenic growth and organization rather than fibrogenic growth due to the abundance of myofibers and decrease in ECM. Ultimately, the increase in protein synthesis suggests that the SMUs administered 25 nM DEX at early differentiation were beginning to develop more myofibers and sarcomeric organization, which may produce more advanced structural properties than SMUs with sustained administration of 10 nM DEX if provided more time to develop. Overall, sustained administration of 10 nM DEX (days 0–16) improved myogenic differentiation and structural maturation, yielding SMUs with the greatest force production.

Evaluation of the contractile properties of our SMUs showed that isometric force production was enhanced with administration of 25 nM DEX at early differentiation (days 5–7) and sustained administration of 10 nM DEX (days 0–16); however, no differences were found between the DEX-receiving groups with TPT and ½ RT. Consequently, our data suggests that the timing and dose of DEX supplemented to our SMUs does not play a significant role in the calcium dynamics. However, it has been shown that changes in serum origin, glucose concentration, and electrical stimulation alter key determinants of TPT and ½ RT, such as myosin heavy chain, troponin, and SERCA isoforms [Khodabukas and Baar, 2014; Khodabukas and Baar, 2015; Dennis et al., 2001; Huang et al., 2006]. Based on our previous study showing enhanced function with DEX addition, these findings of altered time-dependent contractile properties with growth factors suggest that further investigation should be done to determine whether or not the administration of DEX effects these parameters.

Ultimately, in our DEX-receiving SMUs, it would be beneficial to measure the expression levels of proteins responsible for calcium release and re-uptake in muscle to determine if DEX administration to our SMUs changes the expression of these proteins that correlate to calcium dynamics. Subsequently, whether these changes at the protein level have functional consequences could be confirmed.

The administration of sustained 10 nM DEX advanced myogenesis and structural maturation, which supported the results observed in our previous evaluation of DEX. Though, in comparison to our previous results, sustained administration of 10 nM DEX produced an average isometric tetanic force 73.7% greater than the average isometric tetanic force produced with sustained administration of 10 nM DEX in this study (256.5 μN versus 147.7 μN, respectively) [Syverud et al., 2016]. It is important to note that in this study, sustained administration of 10 nM DEX exhibited a large variation in the forces measured in constructs from different cell isolations; comparison of forces between isolations showed a range of tetanic forces from 50.7 μN to 270.5 μN. Potential explanations for the considerable variation in tetanic force are the differences in purity of satellite cell population at the time of seeding. Therefore, we are currently developing techniques to increase the purity of the percentage of satellite cells in our starting cell source to subsequently reduce variability in construct fabrication times and outcomes such as force production. In particular, it is important to force test the constructs when they are composed of mature and aligned myofibers, since contractile function of the construct is determined by the muscle architecture.

Furthermore, with sustained administration of 25 nM DEX the cells exhibited extensive membrane blebbing, a biomarker for apoptosis [Syverud et al., 2016; Ward et al., 2008]. While sustained administration of 25 nM DEX appeared to produce a toxic environment, single dose administration of 25 nM DEX during a precise stage of myogenesis reduced the amount of blebbing, yet is insufficient to produce optimal SMUs with respect to structural maturity and functionality. Further analysis is necessary to assess the source of blebbing and to determine if administration of 25 nM DEX at more than one time point of our fabrication process could produce SMUs with more advanced sarcomeric structure and higher force production. Specifically, SMUs with the most advanced structure and function may be produced from administration of 10 nM DEX continuously with administration of 25 nM DEX during early differentiation (days 5–7), or administration of 10 nM DEX continuously with administration of 25 nM DEX during the majority of early proliferation (days 0–3) and early differentiation (days 5–7). Overall, these observations reinforce the importance of developing a strict methodology for engineering skeletal muscle.

In conclusion, we found that altering the timing of 25 nM DEX administration did not enhance the overall structure or function of our SMUs, and SMUs were optimally fabricated with sustained administration of 10 nM DEX. Overall, supplementation of DEX to our muscle isolates *in vitro* has improved our skeletal muscle fabrication protocol by enhancing myogenesis, structural maturation, and force production of our SMUs developing more adult-like muscle. Future studies will utilize 10 nM DEX and examine the effects of other growth factors with myogenic potential *in vitro*.

Acknowledgements

The authors would like to acknowledge contributions by Alejandro Moncada, as well as the support of the NIH/NIAMS 1R01AR067744-01, internal funding from the Rackham Graduate School, University of Michigan, and the University of Michigan Microscopy, Imaging & Analysis Laboratory (MIL).

Abbreviations used in this paper

ABAM	antibiotic-antimycotic
DEX	dexamethasone
DPBS	Dulbecco's phosphate-buffered saline
DMEM	Dulbecco's modified Eagle's medium
ECM	extracellular matrix
FBS	fetal bovine serum
ICC	Immunocytochemistry
MDM	muscle differentiation medium
MGM	muscle growth medium
PBS	phosphate-buffered saline
RER	rough endoplasmic reticulum
SMUs	skeletal muscle units
TEM	transmission electron microscope
TPT	time to peak
VML	volumetric muscle loss
½ RT	half relaxation time

References

Allen RE, Boxhorn LK (1989) Regulation of skeletal muscle satellite cell proliferation and differentiation by transforming growth factor-beta, insulin-like growth factor I, and fibroblast growth factor. J Cell Physiol 138: 311–315. [PubMed: 2918032]

Alway SE, Pereira SL, Edens NK, Hao Y, Bennett BT (2013) β-Hydroxy-β-methylbutyrate (HMB) enhances the proliferation of satellite cells in fast muscle of aged rats during recovery from diuse atrophy. Exp Geront 48: 973–984.

Belanto JJ, Diaz-Perez SV, Magyar CE, Maxwell MM, Yilmaz Y, Topp K, Boso G, Jamieson CH, Cacalano NA, Jamieson CAM (2010) Dexamethasone induces dysferlin in myoblasts and enhances their myogenic differentiation. Neuromuscul Disord 20: 111–121. [PubMed: 20080405]

Dennis RG, Kosnik PE, Gilbert ME, Faulkner JA (2001) Excitability and contractility of skeletal muscle engineered from primary cultures and cell lines. Am J Physiol Cell Physiol 280: 288–295.

Dennis RG, Kosnik PE (2000) Excitability and isometric contractile properties of mammalian skeletal muscle constructs engineered *in vitro*. In Vitro Cell Dev Biol Anim 36: 327–335. [PubMed: 10937836]

Desler MM, Jones SJ, Smith CW, Woods TL (1996) Effects of dexamethasone and anabolic agents on proliferation and protein synthesis and degradation in C2C12 myogenic cells. J Anim Sci 74: 1265–1273. [PubMed: 8791198]

Giorgino F, Smith RJ (1995) Dexamethasone enhances insulin-like growth factor-1 effects on skeletal muscle cell proliferation. J Clin Invest 96: 1473–1483. [PubMed: 7544807]

Morgan SA, Hassan-Smith ZK, Doig CL, Sherlock M, Stewart PM, Lavery GG (2016) Glucocorticoids and 11β-HSD1 are major regulators of intramyocellular protein metabolism. J Endocrinol 229: 277–286. [PubMed: 27048233]

Huang YC, Dennis RG, Baar K (2006) Cultured slow vs. fast skeletal muscle cells differ in physiology and responsiveness to stimulation. Am J Physiol Cell Physiol 291: 11–17.

Husmann I, Soulet L, Gautron J, Martelly I, Barritault D (1996) Growth factors in skeletal muscle regeneration. Cytokine Growth Factor Rev 7: 249–258. [PubMed: 8971480]

Inder WJ, Jang C, Obeyesekere VR, P Alford F (2010) Dexamethasone administration inhibits skeletal muscle expression of the androgen receptor and IGF-1 – Implications for steroid-induced myopathy. Clin Endocrinol (Oxf) 73: 126–132. [PubMed: 19681914]

Khodabukas A, Baar K (2015) Contractile and metabolic properties of engineered skeletal muscle derived from slow and fast phenotype mouse muscles. J Cell Physiol 230: 1750–1757. [PubMed: 25335966]

Khodabukas A, Baar K (2014) The effect of serum origin on tissue engineered skeletal muscle function. J Cell Biochem 115: 2198–2207. [PubMed: 25146978]

Kuo T, Lui PH, Chen T, Lee RA, New J, Zhang D, Lei C, Chau A, Tang Y, Cheung E, Wang J (2016) Transcriptional regulation of FoxO3 gene by glucocorticoids in murine myotubes. Am J Physiol Endocrinol Metab 310: 572–585.

Larkin LM, Kuzon WM Jr., Supiano MA, Galecki A, Halter JB (1998) Effect of age and neurovascular grafting on the mechanical function of medial gastrocnemius muscles of Fischer 344 rats. J Gerontol A Biol Sci Med Sci 53: B252–258. [PubMed: 18314554]

Larkin LM, Calve S, Kostrominova TY, Arruda EM (2006) Structure and functional evaluation of tendon-skeletal muscle constructs engineering *in vitro*. Tissue Eng 12: 3149–3158. [PubMed: 17518629]

Mertens JP, Sugg KB, Lee JD, Larkin LM (2014) Engineering muscle constructs for the creation of functional engineered musculoskeletal tissue. Regen Med 9: 89–100. [PubMed: 24351009]

National Research Counsil (1996) Guide for the care and use of laboratory animals. The National Academics Press: Washington, DC.

Qin J, Du R, Yang Y, Zhang H, Li Q, Liu L, Guan H, Hou J, An X (2013) Dexamethasone-induced skeletal muscle atrophy was associated with upregulation of myostatin promoter activity. Res Vet Sci 94: 84–89. [PubMed: 22939086]

Schakman O, Gilson H, Thissen JP (2008) Mechanisms of glucocorticoid-induced myopathy. J Endocrinol 197: 1–10. [PubMed: 18372227]

Syverud BC, VanDusen KW, Larkin LM (2016) Effects of dexamethasone on satellite cells and tissue engineered skeletal muscle units. Tissue Eng Part A 22: 480–490. [PubMed: 26790477]

VanDusen KW, Syverud BC, Williams ML, Lee JD, Larkin LM (2014) Engineered skeletal muscle units for repair of volumetric muscle loss in the tibialis anterior muscle of a rat. Tissue Eng Part A 20: 2920–2930. [PubMed: 24813922]

Ward TH, Cummings J, Dean E, Greystroke A, Hou JM, Backen A, Ranson M, Dive C (2008) Biomarkers of apoptosis. Br J Cancer 99: 841–846. [PubMed: 19238626]

Williams ML, Kostrominova TY, Arruda EM, Larkin LM (2013) Effects of implantation on engineered skeletal muscle constructs. J Tissue Eng Regen Med 7: 434–442. [PubMed: 22328229]

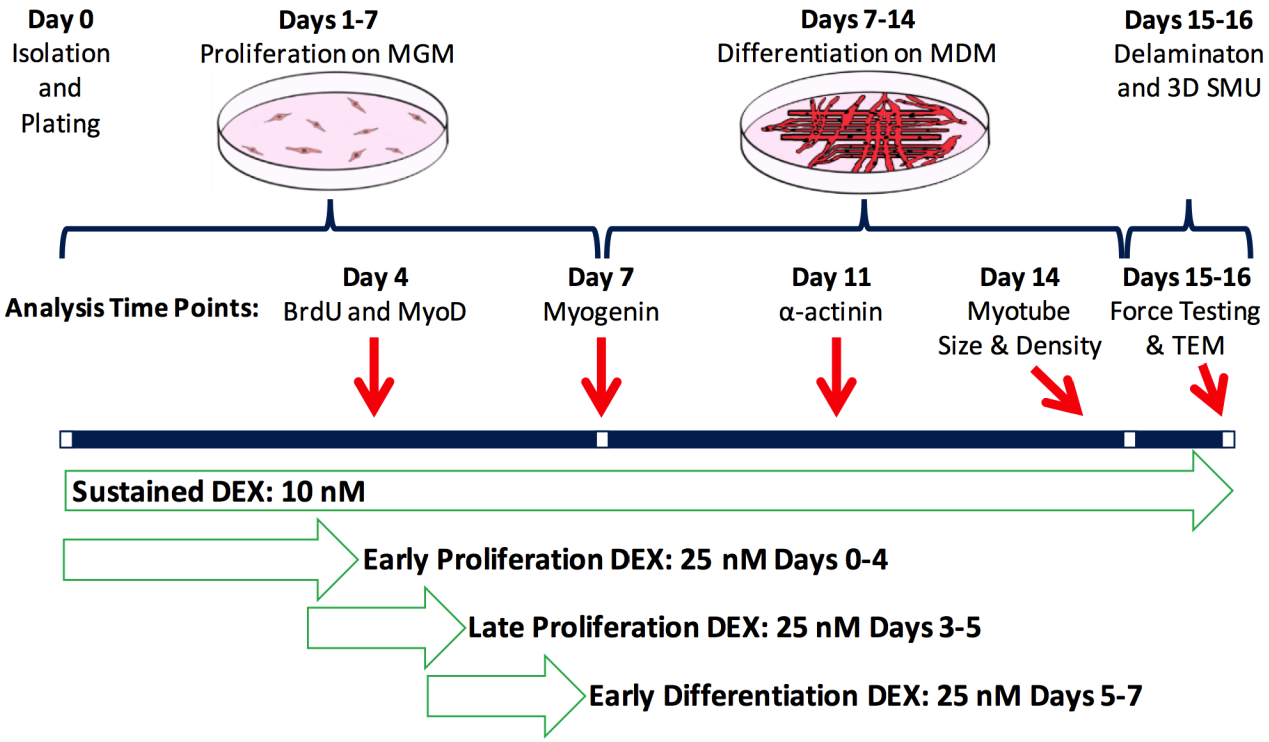

Figure 1:

Experimental Timeline. To study the effects of DEX on the early and late stages of proliferation and early stage of differentiation, DEX was supplemented from days 0–4, days 3–5, and days 5–7 at a 25 nM dose. Sustained addition of 10 nM DEX, which showed optimal SMU function in our previous study, was used as a control. Throughout the SMU fabrication process, myogenesis was analyzed with immunostaining for proliferation with BrdU and MyoD, differentiation with myogenin, myotube fusion and structural maturation with α-actinin, and myotube size and density with light microscopy. Following 3-D SMU formation, isometric tetanic force production was measured to assess functionality. MGM stands for Muscle Growth Medium, MDM for Muscle Differentiation Medium.

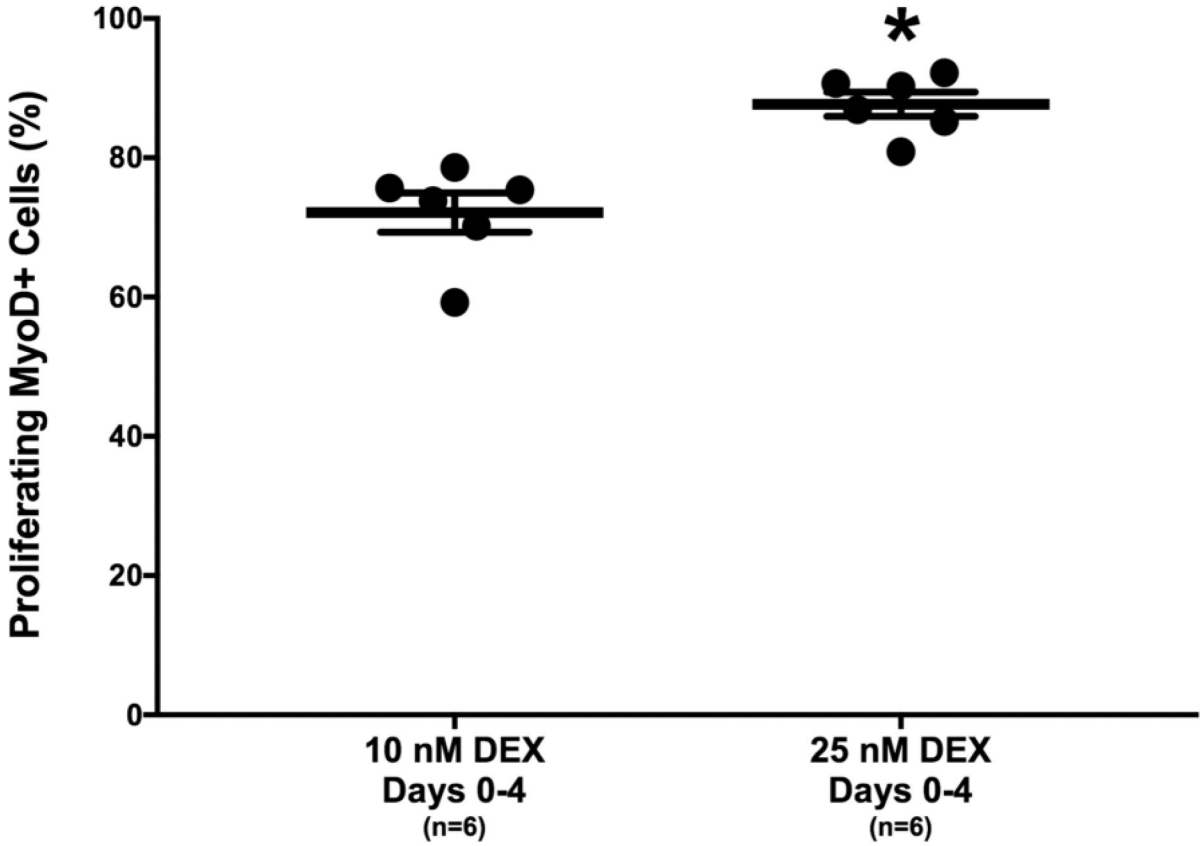

Figure 2:

DEX Effects on Myogenic Proliferation. Percentage of proliferating cells expressing MyoD, indicated by BrdU and MyoD co-staining on day 4. Myogenic proliferation was significantly greater with early administration of 25 nM DEX compared to sustained 10 nM DEX ($p<0.001$). Thick bars show the mean; error bars indicate standard error. *Indicates a significant difference from sustained 10 nM DEX.

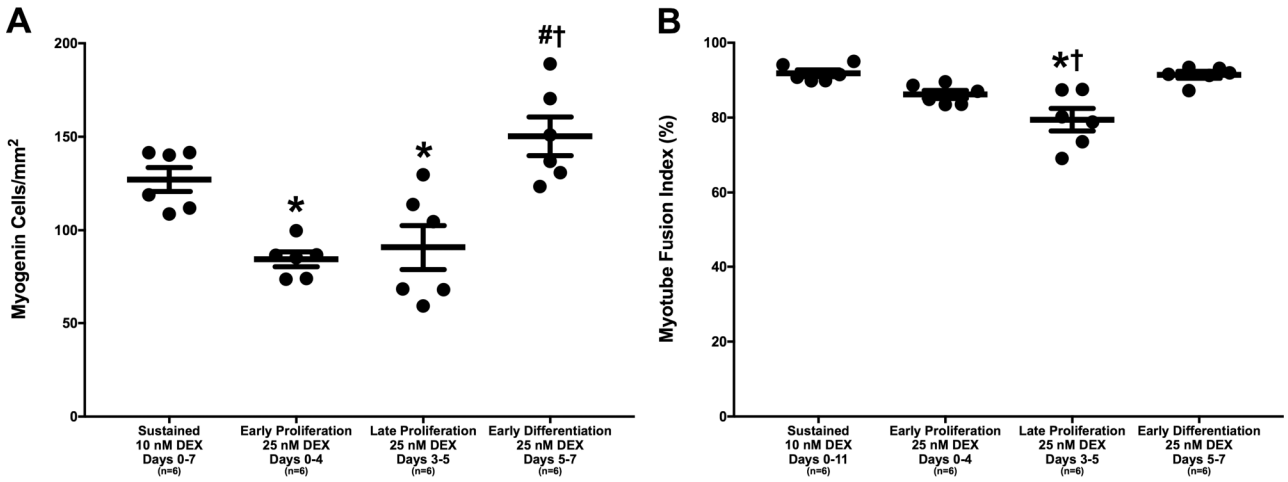

Figure 3:

DEX Effects on Myoblast Differentiation into Myotubes. (A) Myogenin-positive cell density, indicating fusion of myoblasts into myotubes, observed with myogenin immunostaining on day 7. Myogenin-positive cell density was significantly lower with administration of 25 nM at early and late stages of proliferation compared to sustained administration of 10 nM DEX and administration of 25 nM DEX at early differentiation ($p=0.012$, $p=0.036$, $p<0.001$, and $p<0.001$, respectively). (B) Myotube fusion index, representing the percentage of myonuclei associated with a myotube containing 4 or more myonuclei, determined from α-actinin and DAPI staining on day 11. *Post hoc* analysis indicates a significantly lower myotube fusion index with administration of 25 nM DEX at late proliferation compared to both sustained administration of 10 nM DEX and administration of 25 nM DEX at early differentiation ($p<0.001$ for both). Thick bars show the mean; error bars indicate standard error. *Indicates a significant difference from sustained 10 nM DEX, †from late proliferation 25 nM DEX.

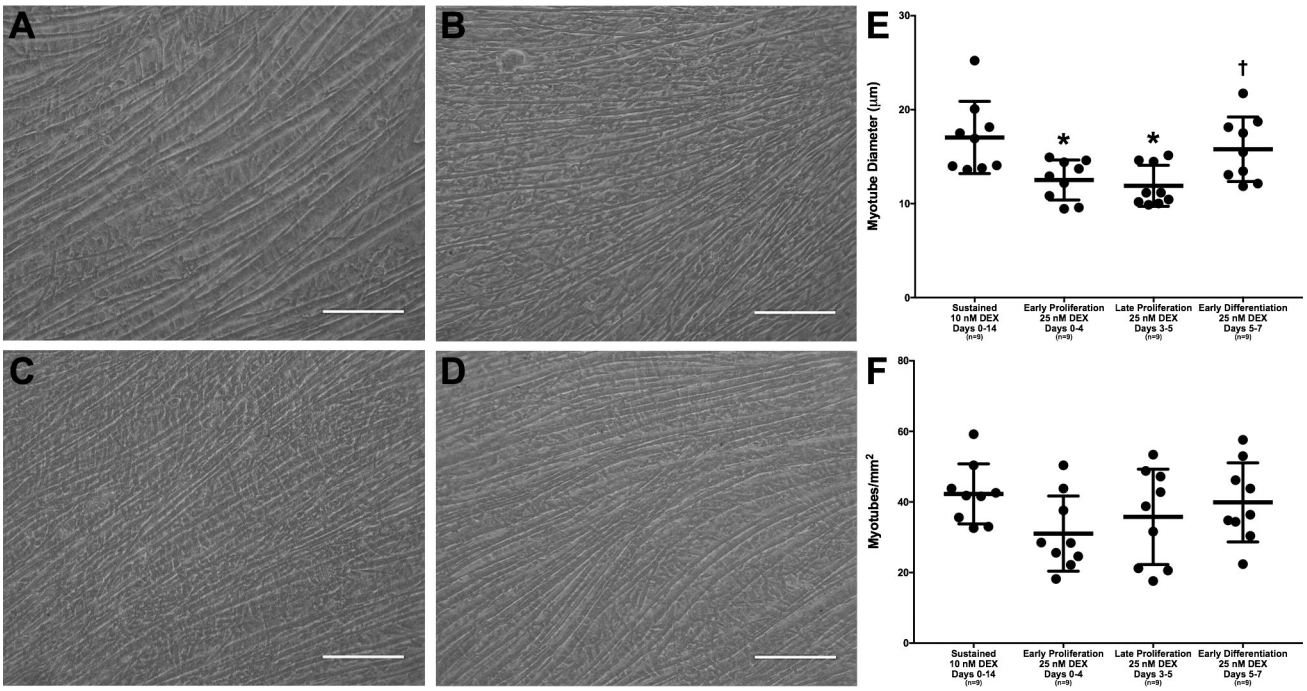

Figure 4:

DEX Effects on Myotube Size and Density. Light microscopy images of monolayers were observed before monolayer delamination on day 14. Representative images are shown above for (A) sustained administration of 10 nM DEX (days 0–14), administration of 25 nM DEX at (B) early proliferation (days 0–4), (C) late proliferation (days 3–5), and (D) early differentiation (days 5–7). All images were analyzed for (E) myotube diameter and (F) myotube density. ImageJ analysis indicates that the average myotube diameter is significantly lower with administration of early and late proliferation 25 nM DEX compared to sustained 10 nM DEX ($p=0.015$ and $p=0.005$, respectively). Comparison of 25 nM DEX-receiving groups indicates that the average myotube diameter produced through the administration of 25 nM DEX at late proliferation was significantly lower than that produced with administration of 25 nM DEX at early differentiation ($p=0.045$). There were no significant differences found between the myotube density of the four groups. Scale bars = 100 μm. Thick bars show the mean; error bars indicate standard error. *Indicates a significant difference from sustained 10 nM DEX, †from late proliferation 25 nM DEX.

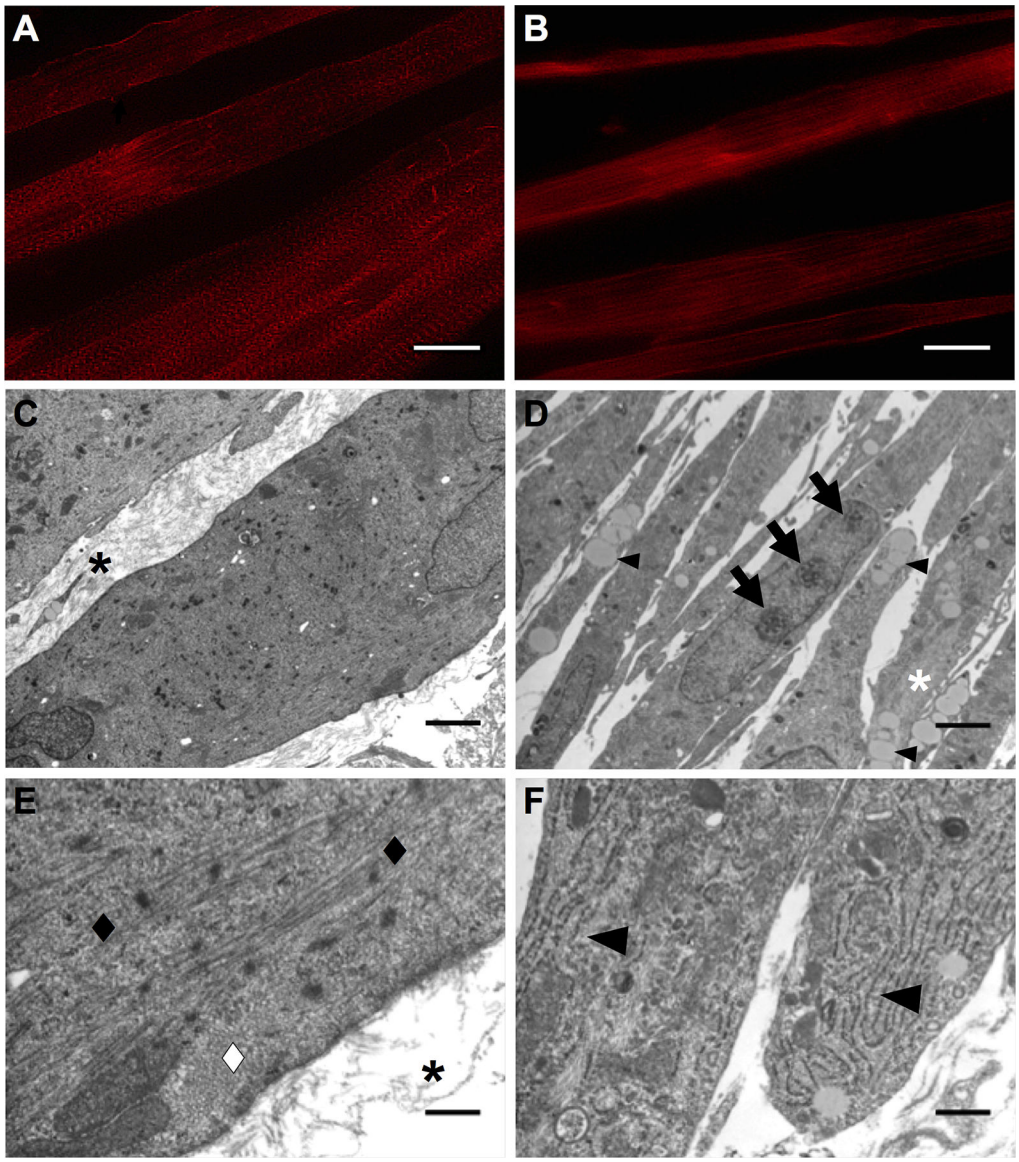

Figure 5:

DEX Effects on SMU Structural Maturation. Representative images of α-actinin immunostaining on day 11 following (A) sustained administration of 10 nM DEX (days 0–11) and (B) administration of 25 nM DEX at early differentiation (days 5–7). The greatest advancement in sarcomeric structure and alignment of muscle fibers was observed with sustained administration of 10 nM DEX. Transmission electron micrographs of longitudinal sections of SMUs following (C, E) sustained administration of 10 nM DEX (days 0–16) and (D, F) administration of 25 nM DEX at early differentiation (days 5–7). Sustained administration of 10 nM DEX images show larger myofibers with an abundance of collagen ECM between myofibers, indicated by black asterisks in (C, E), while administration of 25 nM DEX at early differentiation images show smaller myofibers and the absence of collagen ECM between myofibers. Black and white diamonds in (E) indicate sarcomeres in longitudinal and cross orientation along the length of the myofibers observed with sustained

administration of 10 nM DEX, respectively. No sarcomeres were observed with administration of 25 nM DEX at early differentiation, but TEM images showed an abundance of myofilaments, lipids droplets, and nucleoli in myonuclei, indicated by a white asterisk, small arrowheads, and arrows in (D), respectively. In addition, large arrowheads in (F) indicate an increase in rough endoplasmic reticulum in the cytoplasm of myocytes with administration of 25 nM DEX at early differentiation. Scale bars in (A, B) 20 μm, (C, D) 2 μm, (E, F) 400 nm.

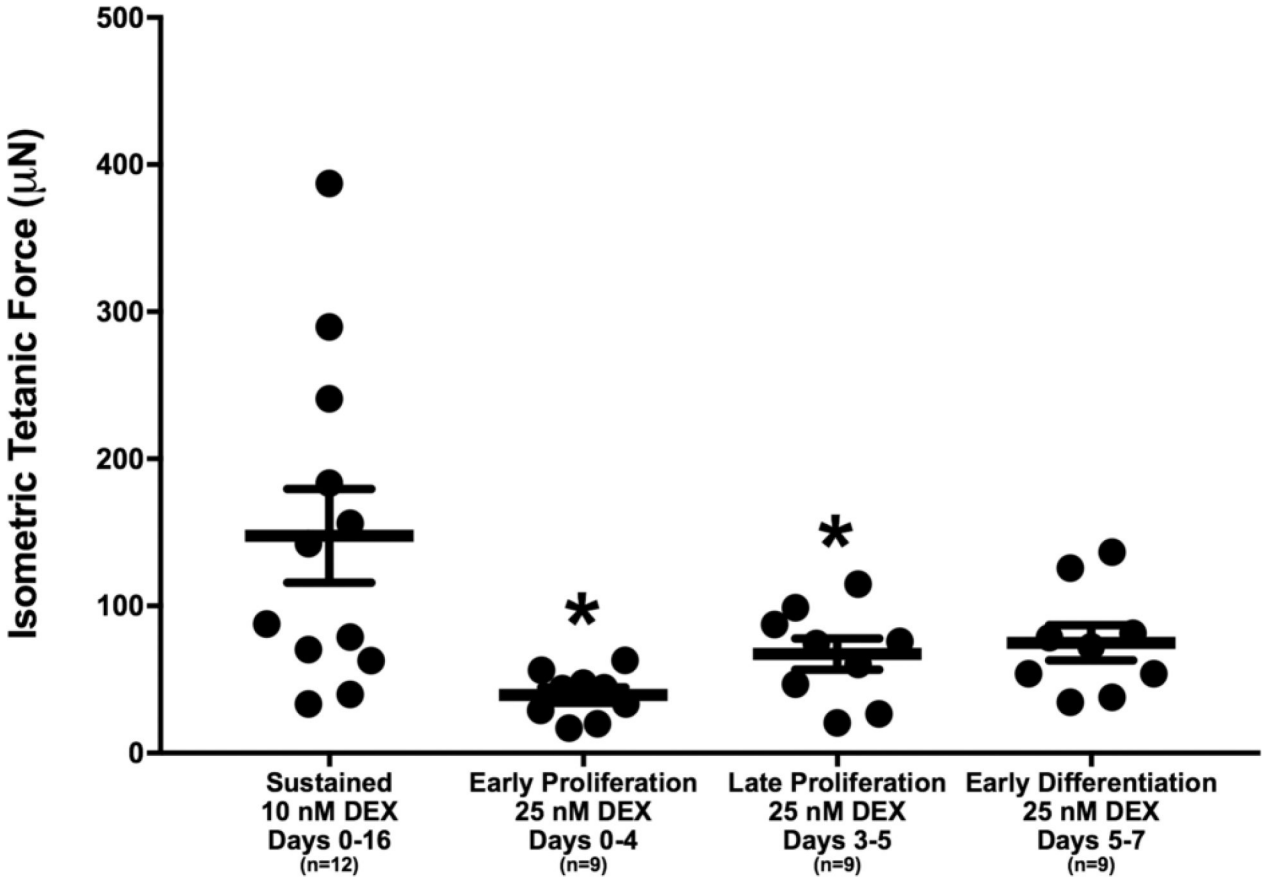

Figure 6:

DEX Effects on Force Production. Functional properties 70 of 3-D SMUs assessed on days 15–16 by measuring isometric tetanic force production following electrical stimulation. SMUs with administration of 25 nM DEX at early and late stages of proliferation exhibited average maximum forces significantly lower than SMUs receiving sustained administration of 10 nM DEX ($p=0.004$ and $p=0.045$, respectively). There were no significant differences in average maximum isometric forces within the 25 nM DEX-receiving cohorts. Thick bars show the mean, and error bars indicate standard error. *Indicates a significant difference from sustained 10 nM DEX.

Table 1.

Comparison of contractile properties of DEX-supplemented SMUs.

	TPT (ms)	½ RT (ms)
Sustained 10 nM DEX Days 0–16	476.3 ± 37.0	334.7 ± 19.5
Early Proliferation 25 nM DEX Days 0–4	584.0 ± 93.0	397.0 ± 39.8
Late Proliferation 25 nM DEX Days 3–5	489.3 ± 68.9	337.0 ± 16.6
Early Differentiation 25 nM DEX Days 5–7	545.3 ± 11.3	334.7 ± 19.5

Values at mean ± SEM. Abbreviations: TPT, Time to Peak Tension; ½ RT, Half Relaxation Time.